

# Small Size Effects in Open and Closed Systems: What Can We Learn from Ideal Gases about Systems with Interacting Particles?

Vilde Bråten,<sup>1</sup> Dick Bedeaux,<sup>2</sup> Øivind Wilhelmsen,<sup>2</sup> and Sondre Kvalvåg Schnell<sup>1, a)</sup>

<sup>1</sup>*Department of Materials Science and Engineering, Norwegian University of Science and Technology, NTNU, Trondheim, NO-7491, Norway*

<sup>2</sup>*PoreLab, Department of Chemistry, Norwegian University of Science and Technology, NTNU, Trondheim, NO-7491, Norway*

(Dated: 7 December 2021)

Small systems have higher surface area-to-volume ratios than macroscopic systems. One consequence of this is that properties of small systems can be dependent on the system's ensemble. By comparing the properties in grand canonical (open) and canonical (closed) systems, we investigate how a small number of particles can induce an ensemble dependence. The ensemble equivalence of small ideal gas systems is investigated by deriving the properties analytically, while the ensemble equivalence of small systems with particles interacting via the Lennard-Jones or the Weeks-Chandler-Andersen potential is investigated through Monte Carlo simulations. For all investigated small systems, we find clear differences between the properties in open and closed systems. For systems with interacting particles, the difference between the pressure contribution to the internal energy, and the difference between the chemical potential contribution to the internal energy, are increasing with system size and number density. The difference in chemical potential is, with the exception of the density dependence, qualitatively described by the analytic formula derived for an ideal gas system. The difference in pressure, however, is not captured by the ideal gas model. For the difference between the properties in the open and closed systems, the response of increasing the particles' excluded volume is similar to the response of increasing the repulsive forces on the system walls. This indicates that the magnitude of the difference between the properties in open and closed systems is related to the restricted movement of the particles in the system.

## I. INTRODUCTION

The effect a system's finite size can have on its properties is an important factor to consider when investigating systems through simulations<sup>1</sup>. Initially, finite size effects in simulations were unwanted, since the main goal of the simulations was to extract macroscopic properties. Research on finite size effects was therefore mainly focused on finding corrections for them, so that the properties in the thermodynamic limit could be extracted. In addition to the numerous theoretical descriptions<sup>2-8</sup>, finite size effects have been investigated to a large extent through simulations for both simple model fluids, and for complex molecular fluids<sup>9-20</sup>.

With increased interest in nanosized systems in fields such as biology<sup>21,22</sup>, atmospheric science<sup>23</sup> and porous media science<sup>24,25</sup>, it becomes important to understand how these finite size effects are not only artifacts in simulations, but significant contributions to the behavior of small systems. In naturally occurring nanosized systems, the small size effect is an inherent part of the system. To get a complete understanding of the behavior of such systems, we need a proper description of the finite size effects. An essential part of this development is to have a thermodynamic description that applies on a small size scale. This was provided by Hill<sup>26</sup> through an extension of classical thermodynamics that can be applied to small systems, often referred to as nanothermodynamics. Nanothermodynamics has been used in different works to describe small systems, like in the description of transport in porous

media<sup>27,28</sup>, stretching and breaking of polymer chains<sup>29,30</sup>, and in the use of sub-sampling techniques for computation of macroscopic thermodynamic properties<sup>14,19,20</sup>.

The objective of this paper is to demonstrate how investigations of a simple model system can be used in combinations with Hill's<sup>26</sup> nanothermodynamics to gain more insight into the behavior of small systems. More specifically, we investigate whether small confinement can lead to a difference in the properties of open and closed system. We consider single-phase systems that are inherently identical except for their boundaries. The open system considered here is in the grand canonical ensemble, and can exchange particles and energy with the surroundings, while the closed system is in the canonical ensemble and can exchange only energy with the surroundings.

If the two ensembles predict compatible or equivalent equilibrium states for a given system, we refer to this system as ensemble equivalent<sup>31,32</sup>. In classical thermodynamics, it is well known that ensemble equivalence holds for macroscopic systems with short range interactions. However, it is also known that systems with a small number of particles can be ensemble *in-equivalent*. This can occur when properties that are regarded extensive in the thermodynamic limit are influenced by finite size effects and become non-extensive. It is not surprising that Hill's<sup>26</sup> formalism, where the thermodynamic properties have been derived for each ensemble separately, has gained some interest in the research on ensemble in-equivalence. Rubi, Bedeaux, and Kjelstrup<sup>33</sup> used Hill's<sup>26</sup> framework in a theoretical investigation of the properties of a single molecule under isomeric and isotensional conditions<sup>33</sup>. Bering *et al.*<sup>29</sup> later showed that the in-equivalence between these two ensembles can be detected in simulations of poly-

---

<sup>a)</sup>Electronic mail: sondre.k.schnell@ntnu.no

mer chains.

Systems with a large number of particles can also be ensemble in-equivalent. A substantial amount of the research done on ensemble in-equivalence have focused on systems with long-range interactions<sup>31,32,34-36</sup>. The main interest of these studies has been the non-additive, rather than the non-extensive nature of the system's properties. Additivity is closely related to extensivity, but their definitions are different. A thermodynamic property  $f$  is *extensive* if it is Euler homogeneous of degree one with respect to the variable  $x$ , meaning that  $f(2x) = 2f(x)$ . If a property  $f$  is *additive*, it means that if the total system is split into  $i$  sub-parts, the total property is the sum of all its sub-parts,  $f_{\text{tot}} = f_1 + f_2 + \dots + f_i$ . If a property is non-additive, there is an additional contribution from the interaction between the sub-parts,  $f_{\text{int}}$ . This means that a system can be non-additive and still be extensive, if the contribution from the interactions scales with system size<sup>31</sup>. Hence, additive properties are always extensive, and non-extensive properties are non-additive, but not necessarily the other way around. This was used by Campa *et al.*<sup>36</sup> who showed how Hill's<sup>26</sup> nanothermodynamics can be applied to macroscopic, non-additive systems.

Models based on statistical mechanics can provide insight into the mechanisms behind ensemble in-equivalence. In this work, the ideal gas model represents an important case because it has no inter-particle interactions. Studying the ideal gas can possibly reveal ensemble in-equivalence arising from other sources than long-range interactions. Another motivation for studying ideal gases is that previous investigations of their finite size effects have been shown to also apply to systems with interacting particles<sup>13,37,38</sup>.

When investigating model systems with a small number of particles, it is important to keep in mind that some ingrained definitions and relations from statistical mechanics use approximations based on the assumptions that  $N \rightarrow \infty$ , where  $N$  is the number of particles. One example is the proof of the virial theorem, for which Tuckerman<sup>39</sup> briefly discusses the necessary assumption made about the number of microstates associated with different ensembles. The equipartition theorem has also been shown to break down for small particle numbers in systems containing hard spheres<sup>40</sup>, and later for particles interacting via intermolecular potentials<sup>41,42</sup>. Miranda<sup>43</sup> showed that avoiding assumptions about the magnitude of  $N$  in the derivation of the properties of small clusters of harmonic oscillators, and for two level systems, results in differences between the properties in the canonical, micro-canonical and grand canonical ensembles.

Approximations based on the assumption that  $N \rightarrow \infty$  are also used in the classical derivation of the bulk properties of the ideal gas. In this paper, we derive the properties of an ideal gas in a small system with a surface energy, without assuming that  $N \rightarrow \infty$ , and investigate how finite size contributions to the thermodynamic properties arise when the system is small. We find that some finite size terms arise from surface effects, and some arise from avoiding approximations about the magnitude of the number of particles. Similar models have been used previously to investigate ideal gas mixtures with surface energy<sup>44</sup>, and the adsorbed phase on a spherical adsorbent<sup>45</sup>.

Here we take it one step further by presenting a direct comparison of the properties in an open and closed system. We also compare the results of the ideal gas with results from Monte Carlo (MC) simulations of system with Lennard-Jones (LJ) particles, and Weeks-Chandler-Andersen (WCA) particles.

## II. THERMODYNAMICS OF SMALL SYSTEMS

Finite size effects in small systems are usually a result of surface area-to-volume ratios larger than those of macroscopic systems. For small systems, the effects of the surface can be a significant contribution to the thermodynamic properties. As a consequence of this, properties that normally are regarded as extensive in macroscopic systems can become higher order functions of size and shape in small systems. While properties that normally are regarded as intensive in macroscopic systems can become size dependent if the system is small<sup>26</sup>.

The classical macroscopic thermodynamic equations cannot be used to describe the properties in small systems, but the framework developed by Hill<sup>26</sup> provides an extension of the systematic structure of thermodynamics that applies to small systems. Instead of considering one single, small system, Hill<sup>26</sup> investigated a collection of small systems that are all equivalent, distinguishable, and independent. By introducing a new extensive variable  $\mathcal{N}$ , equal to the number of small system replicas, the differential energy of the collection of small systems can be expressed as

$$dU_t = TdS_t - pdV_t + \sum_{i=1}^n \mu_i dN_{i,t} + \mathcal{E}d\mathcal{N}, \quad (1)$$

where  $U_t$  is the energy,  $T$  is temperature,  $S_t$  is entropy,  $p$  is pressure,  $V_t$  is the volume,  $\mu_i$  the chemical potential of component  $i$  and  $N_{i,t}$  the number of particles of component  $i$ , where subscript  $t$  stands for the total collection of small system replicas. The property  $\mathcal{E}$  is called the subdivision potential, and represents the change in  $U_t$  as we change the number of replicas at constant  $S_t$ ,  $V_t$  and  $N_{i,t}$ . From this starting point, Hill retrieve the properties of a single small system by computing the averages of the total collection of small system replicas.

A key part of this derivation is that each thermodynamic ensemble is considered separately. As a consequence, the expression for the subdivision potential takes different forms for the different ensembles, which in turn gives rise some unique small system properties. In the canonical ensemble the subdivision potential is

$$\mathcal{E}(N, V, T) = F(N, V, T) + p(N, V, T)V - \mu(N, V, T)N, \quad (2)$$

while in the grand canonical ensemble it is represented by

$$\mathcal{E}(\mu, V, T) = \Upsilon(\mu, V, T) + p(\mu, V, T)V. \quad (3)$$

The subdivision potential in grand canonical systems is also connected to one of the unique small system properties through  $\mathcal{E}(\mu, V, T) = (p - \hat{p})V$ , where  $\hat{p}$  is known as the integral pressure. For more details on the derivation of these properties we refer to the books by Hill<sup>46</sup>, or the extended explanations presented by Bedeaux, Kjelstrup, and Schnell<sup>44</sup>.

### III. IDEAL GAS IN A SMALL SYSTEM WITH SURFACE ENERGY

In this section, we derive the thermodynamic properties of an ideal gas in a small confinement from the partition function of the system. Many steps of the derivation are based on well known derivations of the properties of an ideal gas<sup>39</sup>. Therefore, only the outlines are provided here, while the full derivation can be found in the Supplementary Material (SM).

In derivations of properties of macroscopic systems, it is normally assumed that  $N \rightarrow \infty$ , which justifies the use of approximations such as Stirling's approximation,  $N! \approx (N/e)^N$ . We will here avoid this assumption, such that the final equations appropriately describe systems with a small number of particles.

#### A. The system

The system we consider here is a three dimensional box with volume equal to  $L^3$ . The ideal gas particles do not interact with each other, but they can interact with the boundaries of the system. This means that the energy of the particles will depend on whether they are located close to the boundary of the system or not. When the particles are closer than a distance  $\delta$  from a wall of the system, they experience a potential energy contribution  $U^s$  from that wall. This means that if a particle is close to an edge, it experiences a potential energy of  $2U^s$ , and if it is close to a corner, it experiences a potential energy of  $3U^s$ . The system, and the different potential energy zones are illustrated in Fig. 1. The potential energy is included in the Hamiltonian through the Heaviside function

$$H(x) = \begin{cases} 0, & \text{if } x < 0 \\ 1, & \text{if } x \geq 0. \end{cases}$$

The Hamiltonian as a function of the particles' momenta  $\mathbf{p}$  and positions  $\mathbf{r}$  then becomes

$$\mathcal{H}(\mathbf{p}, \mathbf{r}) = \sum_{i=1}^N \sum_{\alpha=1}^3 \left( \frac{p_{\alpha i}^2}{2m_i} + U^s [H(\delta - \alpha_i) + H(\alpha_i - (L - \delta))] \right), \quad (4)$$

where  $m$  is the particle mass,  $\beta = 1/k_B T$ , where  $k_B$  is the Boltzmann constant, and  $\alpha = (x, y, z)$  are the Cartesian coordinates.

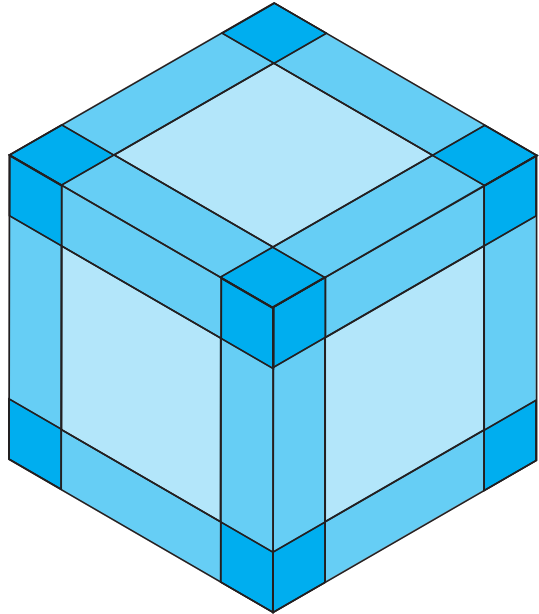


FIG. 1. Illustration of the cubic simulation box with surface energy  $U^s$  experienced by particles closer than a distance  $\delta$  from each wall. Particles close to the sides (light blue regions) experience a potential energy contribution of  $U^s$ , while particles close to the edges (medium blue regions) experience a potential energy contribution of  $2U^s$ , and particles close to the corners (dark blue regions) experience a potential energy contribution of  $3U^s$ .

#### 1. Properties of a confined ideal gas in a closed system

The partition function of the closed system (canonical ensemble), computed from the Hamiltonian in Eq. (4), becomes

$$\begin{aligned} Q(N, V, T) &= \frac{1}{N! h^{3N}} \int_{D(V)} d^N \mathbf{r} d^N \mathbf{p} \exp(-\beta \mathcal{H}(\mathbf{p}, \mathbf{r})) \\ &= \frac{1}{N! h^{3N}} \int_{D(V)} d^N \mathbf{r} \exp \left( -\beta U^s \sum_{i=1}^N \sum_{\alpha=1}^3 [H(\delta - \alpha_i) \right. \\ &\quad \left. + H(\alpha_i - (L - \delta))] \right) \\ &\quad \times \int d^N \mathbf{p} \exp \left( -\beta \sum_{i=1}^N \sum_{\alpha=1}^3 \frac{p_{\alpha i}^2}{2m_i} \right), \quad (5) \end{aligned}$$

where  $h$  is Planck's constant. Since there are no interactions between the particles, the integrals can be split into identical one-dimensional, one-particle integrals. The integral over momenta and the integral over spatial coordinates can be solved separately. The integral over momenta becomes  $1/\Lambda^3$ , where  $\Lambda = \sqrt{h^2 \beta / 2\pi m}$  is the de Broglie wavelength. The one-dimensional, one-particle spatial integral can be split in three parts, where two of these integrals represent the regions that are influenced by the wall potential, and one is the region which is not affected by  $U^s$ .

The final expression for the partition function then becomes

$$Q(N, V, T) = \frac{1}{N!} \left( \frac{L}{\Lambda} \left( 1 - \frac{2\delta}{L} (1 - \exp(-\beta U^s)) \right) \right)^{3N}. \quad (6)$$

It is convenient to express the canonical partition function in terms of the one-particle canonical partition function  $Q(N, V, T) = Q(V, T)^N / N!$ , where  $Q(V, T)$  is

$$Q(V, T) = \frac{V}{\Lambda^3} \left( 1 - \frac{2\delta}{L} (1 - \exp(-\beta U^s)) \right)^3. \quad (7)$$

The properties of a closed system are calculated from the known connection between the partition function and the energy state function. The energy state function of the closed system is the Helmholtz energy, which becomes

$$\begin{aligned} F(N, V, T) &= -k_B T \ln Q(N, V, T) \\ &= k_B T (\ln N! - N \ln Q(V, T)). \end{aligned} \quad (8)$$

The expressions for entropy, pressure and chemical potential are found by differentiating the Helmholtz energy. By combining these identities we can also find the expression for the subdivision potential shown in Eq. (2).

The properties in the closed system are split into three parts, where one represents the well known bulk contribution, another describes the contribution from the surface energy and the last arise from exact treatment of the factorial term,

$$\begin{aligned} \mathcal{A}(N, V, T) &= \mathcal{A}(N, V, T)_{\text{bulk}} + \mathcal{A}(N, V, T)_{\text{surf}} \\ &\quad + \mathcal{A}(N, V, T)_{\text{fac}}. \end{aligned} \quad (9)$$

The different contributions to the thermodynamic properties are presented in Table I, where we assume that the surface energy  $U^s$  is independent of  $N$ ,  $V$  and  $T$  such that its partial derivatives become zero. The complete derivation, as well as the expressions for the thermodynamic properties including the partial derivatives are presented in the SM.

The properties presented in Table I show clear characteristics of small systems. The properties that are regarded as intensive in the thermodynamic limit are size dependent, and the properties that are regarded extensive in the thermodynamic limit are not directly proportional to system size. If  $U^s$  is non-zero, all properties in the closed system become non-extensive due to the  $1/L$  dependence of the surface terms. If  $U^s = 0$ , only the properties that have non-zero factorial terms  $\mathcal{A}(N, V, T)_{\text{fac}} \neq 0$  are influenced by the small number of particles.

## 2. Properties of a confined ideal gas in an open system

The partition function of an open system (grand canonical) is

$$\begin{aligned} \Xi(\mu, V, T) &= \sum_{N=0}^{\infty} \exp(\beta \mu N) Q(N, V, T) \\ &= \sum_{N=0}^{\infty} \frac{(\exp(\beta \mu) Q(V, T))^N}{N!}. \end{aligned} \quad (10)$$

By using  $\exp(a) = \sum_{N=0}^{\infty} a^N / N!$  we get

$$\Xi(\mu, V, T) = \exp(\exp(\beta \mu) Q(V, T)), \quad (11)$$

and the energy state function of the open system is

$$\begin{aligned} \Upsilon(\mu, V, T) &= -k_B T \ln \Xi(\mu, V, T) \\ &= -k_B T \exp(\beta \mu) Q(V, T). \end{aligned} \quad (12)$$

The entropy, pressure and number of particles are calculated from partial derivatives of the energy state function, and the subdivision potential is computed from Eq. (3). From Hill's<sup>26</sup> thermodynamics for small systems we also have the integral pressure  $\hat{p} = -\Upsilon(\mu, V, T)/V$ .

The properties of the open system are represented by three contributions, but in contrast to the closed system, none of these arise from factorial terms. The total properties are given as a sum of a bulk contribution and a surface contribution, which is multiplied with an additional surface contribution

$$\begin{aligned} \mathcal{B}(\mu, V, T) &= \left[ \mathcal{B}(\mu, V, T)_{\text{bulk}} + \mathcal{B}(\mu, V, T)_{\text{surf},1} \right] \\ &\quad \times \mathcal{B}(\mu, V, T)_{\text{surf},2}, \end{aligned} \quad (13)$$

where

$$\mathcal{B}(\mu, V, T)_{\text{surf},2} = \left( 1 - \frac{2\delta}{L} (1 - \exp(-\beta U^s)) \right)^3. \quad (14)$$

The other two contributions to Eq. (13) are presented in Table II, where we again have assumed that the partial derivatives of  $U^s$  are zero.

In contrast to the closed systems, the small size contributions in the open systems are only present if  $U^s$  is non-zero.  $U^s = 0$  means that all size effects vanish, and only the bulk contribution remains.

## B. Comparing properties of a confined ideal gas in open and closed systems

When  $dU^s = 0$ , the properties in the open and closed systems can easily be compared at the same density, meaning that

$$\begin{aligned} \frac{N}{V} &= \frac{N(\mu, V, T)}{V} \\ &= \exp(\beta \mu) \frac{1}{\Lambda^3} \left( 1 - \frac{2\delta}{L} (1 - \exp(-\beta U^s)) \right)^3. \end{aligned} \quad (15)$$

By inserting this expression into the identities shown in Tables I-II we can directly compare the energy state functions, entropy, pressure, chemical potential and subdivision potential of the open and closed systems.

It becomes clear that when the wall potential is independent of the ensemble variables ( $dU^s = 0$ ), the difference between the properties of an ideal gas in the open and closed systems arises from the factorial terms given in the last column in Table I. This means that this difference is simply an effect of a small number of particles, and not an effect of the surface.

TABLE I. Thermodynamic properties of an ideal gas confined in a closed cubic box with surface energy  $U^s$  experienced by all particles within a distance  $\delta$  from each wall.

$\mathcal{A}(N, V, T)$	$\mathcal{A}(N, V, T)_{\text{bulk}}$	$\mathcal{A}(N, V, T)_{\text{surf}}$	$\mathcal{A}(N, V, T)_{\text{fac}}$
$F(N, V, T)$	$Nk_{\text{B}}T \left( \ln \left( \frac{N}{V} \Lambda^3 \right) - 1 \right)$	$-3Nk_{\text{B}}T \ln \left( 1 - \frac{2\delta}{L} (1 - \exp(-\beta U^s)) \right)$	$k_{\text{B}}T \left( \ln N! - N \ln \left( \frac{N}{e} \right) \right)$
$S(N, V, T)$	$Nk_{\text{B}} \left( \ln \left( \frac{V}{N} \frac{1}{\Lambda^3} \right) + \frac{5}{2} \right)$	$Nk_{\text{B}} \left( 3 \ln \left( 1 - \frac{2\delta}{L} (1 - \exp(-\beta U^s)) \right) + \frac{2\delta}{L} \frac{3\beta U^s \exp(-\beta U^s)}{1 - \frac{2\delta}{L} (1 - \exp(-\beta U^s))} \right)$	$-k_{\text{B}} \left( \ln N! - N \ln \left( \frac{N}{e} \right) \right)$
$p(N, V, T)$	$\frac{Nk_{\text{B}}T}{V}$	$\frac{Nk_{\text{B}}T}{V} \left( \frac{2\delta}{L} \frac{1 - \exp(-\beta U^s)}{1 - \frac{2\delta}{L} (1 - \exp(-\beta U^s))} \right)$	—
$\mu(N, V, T)$	$k_{\text{B}}T \ln \left( \frac{N}{V} \Lambda^3 \right)$	$-3k_{\text{B}}T \ln \left( 1 - \frac{2\delta}{L} (1 - \exp(-\beta U^s)) \right)$	$k_{\text{B}}T \left( \frac{1}{N!} \frac{\partial N!}{\partial N} - \ln N \right)$
$\mathcal{E}(N, V, T)$	—	$Nk_{\text{B}}T \left( \frac{2\delta}{L} \frac{1 - \exp(-\beta U^s)}{1 - \frac{2\delta}{L} (1 - \exp(-\beta U^s))} \right)$	$Nk_{\text{B}}T \left( \frac{\ln N!}{N} + 1 - \frac{1}{N!} \frac{\partial N!}{\partial N} \right)$

TABLE II. Thermodynamic properties of an ideal gas confined in an open cubic box with surface energy  $U^s$  experienced by all particles within a distance  $\delta$  from each wall.

$\mathcal{B}(\mu, V, T)$	$\mathcal{B}(\mu, V, T)_{\text{bulk}}$	$\mathcal{B}(\mu, V, T)_{\text{surf},1}$
$\Upsilon(\mu, V, T)$	$-k_{\text{B}}T \exp(\beta\mu) \frac{V}{\Lambda^3}$	—
$S(\mu, V, T)$	$k_{\text{B}} \exp(\beta\mu) \frac{V}{\Lambda^3} \left( \frac{5}{2} - \beta\mu \right)$	$k_{\text{B}} \exp(\beta\mu) \frac{V}{\Lambda^3} \left( \frac{2\delta}{L} \frac{3\beta U^s \exp(-\beta U^s)}{1 - \frac{2\delta}{L} (1 - \exp(-\beta U^s))} \right)$
$p(\mu, V, T)$	$k_{\text{B}}T \exp(\beta\mu) \frac{1}{\Lambda^3}$	$k_{\text{B}}T \exp(\beta\mu) \frac{1}{\Lambda^3} \left( \frac{2\delta}{L} \frac{1 - \exp(-\beta U^s)}{1 - \frac{2\delta}{L} (1 - \exp(-\beta U^s))} \right)$
$N(\mu, V, T)$	$\exp(\beta\mu) \frac{V}{\Lambda^3}$	—
$\mathcal{E}(\mu, V, T)$	—	$k_{\text{B}}T \exp(\beta\mu) \frac{V}{\Lambda^3} \left( \frac{2\delta}{L} \frac{1 - \exp(-\beta U^s)}{1 - \frac{2\delta}{L} (1 - \exp(-\beta U^s))} \right)$
$\hat{p}(\mu, V, T)$	$k_{\text{B}}T \exp(\beta\mu) \frac{1}{\Lambda^3}$	—

The surface effect does change the thermodynamic properties in both systems, meaning that they have different values than they would have in a bulk system, but this surface effect is the same in the open and the closed systems.

The surface energy,  $U^s$ , can in theory depend on temperature, system size, number of particles and chemical potential. Strøm, Bedeaux, and Schnell<sup>45</sup> showed how it is possible to define  $U^s$  such that it depends on the surface area of an adsorbed phase. Since systems with this type of behavior is beyond the scope of this paper, we will not investigate this further here.

All factorial terms in the last column of Table I can be solved in an exact manner using the gamma function and the polygamma function, but approximations can be helpful to

get insight on the form and magnitude of these terms. If we evaluate these terms with the regular Stirling's approximation,  $N! \approx (N/e)^N$ , which normally is used to derive properties in the thermodynamic limit, all factorial terms become zero. We therefore use a more exact version of Stirling's approximation

$$N! \approx \sqrt{2\pi N} \left( \frac{N}{e} \right)^N, \quad (16)$$

which we refer to as "Stirling enhanced". Figure 2 shows that when the number of particles becomes small, it is crucial to compute factorials with a more exact expression than the regular Stirling's approximation. The gamma function is exact also for discrete numbers, but Stirling enhanced is a good rep-

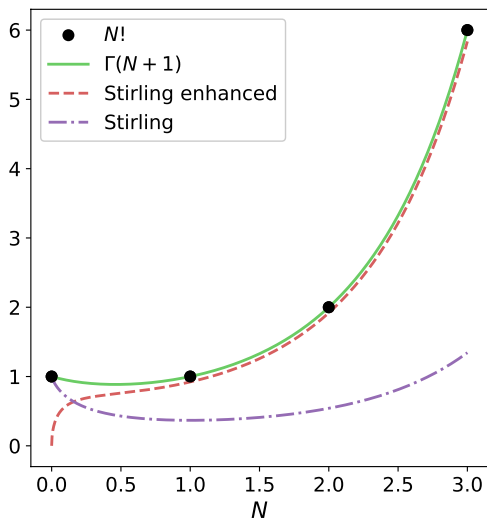


FIG. 2. The factorial computed from exact expressions and approximations.  $\Gamma(N+1)$  represents the gamma function, which gives exact values of the factorial for discrete numbers.

resentation, as long as the average number of particles is larger than one.

Using Eq. (16) results in the following approximations for the factorial terms for the entropy

$$S(N, V, T)_{\text{fac}} = -k_B \left( \ln N! - N \ln \left( \frac{N}{e} \right) \right) \approx -k_B \left( \frac{1}{2} \ln(2\pi N) \right), \quad (17)$$

and the chemical potential

$$\mu(N, V, T)_{\text{fac}} = k_B T \left( \frac{1}{N!} \frac{\partial N!}{\partial N} - \ln N \right) \approx k_B T \left( \frac{1}{2} \frac{1}{N} \right). \quad (18)$$

The factorial contribution to the entropy is clearly increasing with the number of particles, while the factorial contribution to the chemical potential is decreasing with the number of particles.

#### IV. SIMULATION DETAILS

We use an in-house MC code, and all presented values and results are given in reduced LJ units. We investigate systems with particles interacting via two types of potentials:

1. LJ particles interacting via the truncated and shifted potential with the cutoff radius at  $r_c = 2.5$ .
2. Particles interacting through the WCA potential<sup>47</sup>, which is the LJ potential truncated and shifted at  $r_c = 2^{1/6}\sigma$ .

TABLE III. Simulation settings for different boundary conditions (BCs) and interaction potentials (IPs) investigated.  $L$  is the simulation box length,  $T$  represents the temperature,  $n$  represents the number density and  $\mu$  is the chemical potential.

BC	IP	$L$	$T$	$n$	$\mu$
1	LJ	3, 5, 7, 9	3	0.025 - 0.750	-7.0 - 7.5
1	WCA	3, 5, 7, 9	3	0.025 - 0.750	-7.0 - 13.5
2 (a)	LJ	3, 5, 7, 9	3	0.025 - 0.750	-7.0 - 7.5
2 (b)	LJ	3, 5, 7, 9	3	0.025 - 0.750	-4.0 - 10.5
3	LJ	15	3	0.025 - 0.750	-7.0 - 7.5

The simulation boxes are cubic, and we investigate three types of boundary conditions:

1. The particles are confined by a hard wall. This means that the particles do not interact with the walls, but moves attempting to displace a particle outside the walls are rejected.
2. The wall is hard, and the particles closer than a distance  $\delta = 1$  from each wall experience an additional potential energy of (a)  $U^s = 1$  or (b)  $U^s = 3$ .
3. Periodic boundary conditions (PBCs). In order to compare to bulk properties.

The different combinations of simulation settings are presented in Table III.

We run all simulations in five parallels, for  $10^6$  cycles after equilibration. The number of trial moves (i.e. attempts to modify the system) carried out in each cycle has a lower limit of 20, but is otherwise equal to the number of particles. In the closed system, the chemical potential is computed using Widom's<sup>48</sup> test particle insertion method, which is sampled ten times the number of particles in the system, every cycle of the simulation. The pressure in both system types is computed using the virial equation, which is sampled every cycle of the simulation.

#### V. RESULTS AND DISCUSSION

In this section, we present predictions for the ideal gas systems, and the results from the MC simulations of systems with interacting particles.

##### A. Ideal gas

For the ideal gas, the results are computed in systems with  $U^s = 1$  and  $\delta = 1$ , in order to analyze the small size contribution from both the surface terms and the factorial terms. We discuss in detail the ideal gas predictions for system sizes corresponding to the two smallest systems investigated by simulations. Figure 3 shows the energy state functions, entropy, pressure and chemical potential as functions of density for a system with size  $L = 3$ . For the presented densities, a system size of  $L = 3$  corresponds to particle numbers between

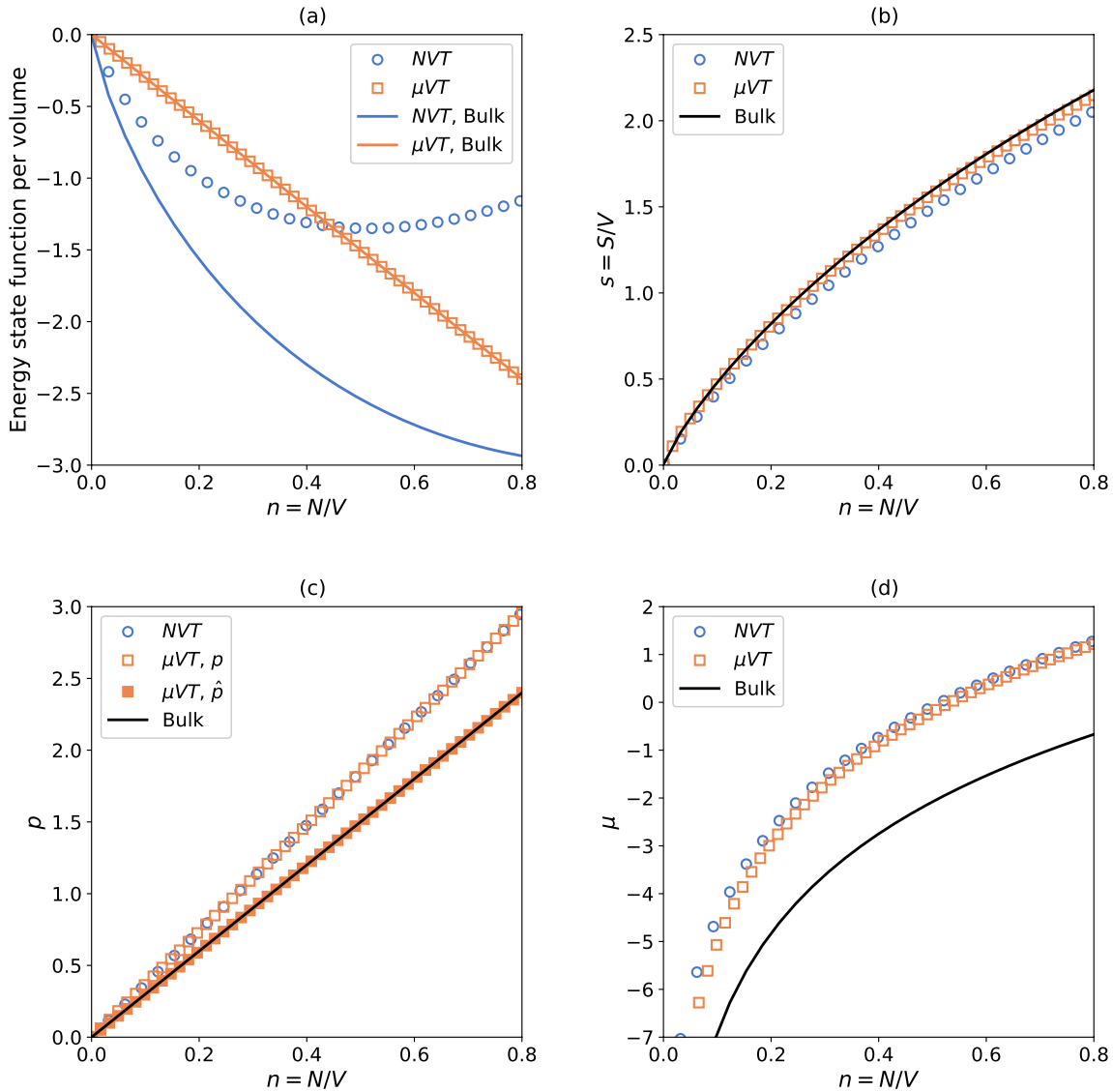


FIG. 3. Energy state functions, entropy, pressure and chemical potential as a function of number density of an ideal gas in a small cubic box with sides  $L = 3$ . The surface energy is  $U^s = 1$  and is experienced by all particles within a distance  $\delta = 1$  from each wall.

approximately 3 and 20. Entropy, pressure and chemical potential show clear deviations from macroscopic values in both the open and the closed systems. The Helmholtz energy in the closed system also shows clear deviations from bulk values. Interestingly, we see that the relationship between  $\Upsilon$  and  $n$  is the same in a small system and in a macroscopic system. Also, the relationship between  $\hat{p}$  and  $n$  in a small system is equal to the relationship between  $p$  and  $n$  in a macroscopic system. A similar result was found for the integral and differential surface tensions of the adsorbed phase investigated by Strøm, Bedeaux, and Schnell<sup>45</sup>. The entropy in the open system is larger than the entropy in the closed system. This was also the case for the properties of the harmonic oscillators

and the two-level systems presented by Miranda<sup>43</sup>, who found a higher entropy for the grand canonical systems than the canonical systems.

Figures 3 (b) and (d) also clearly show the predictions of Eqs. (18) and (17), since the difference between the entropy in the two systems is increasing with density, while the difference between their chemical potentials is decreasing with density. This difference, for both the entropy and the chemical potential, is decreasing as the system becomes larger. Figure 4 shows the energy state functions, entropy, pressure and chemical potential for an ideal gas system with size  $L = 5$ . For the presented densities, this corresponds to particle numbers between approximately 12 and 100. We see that already at

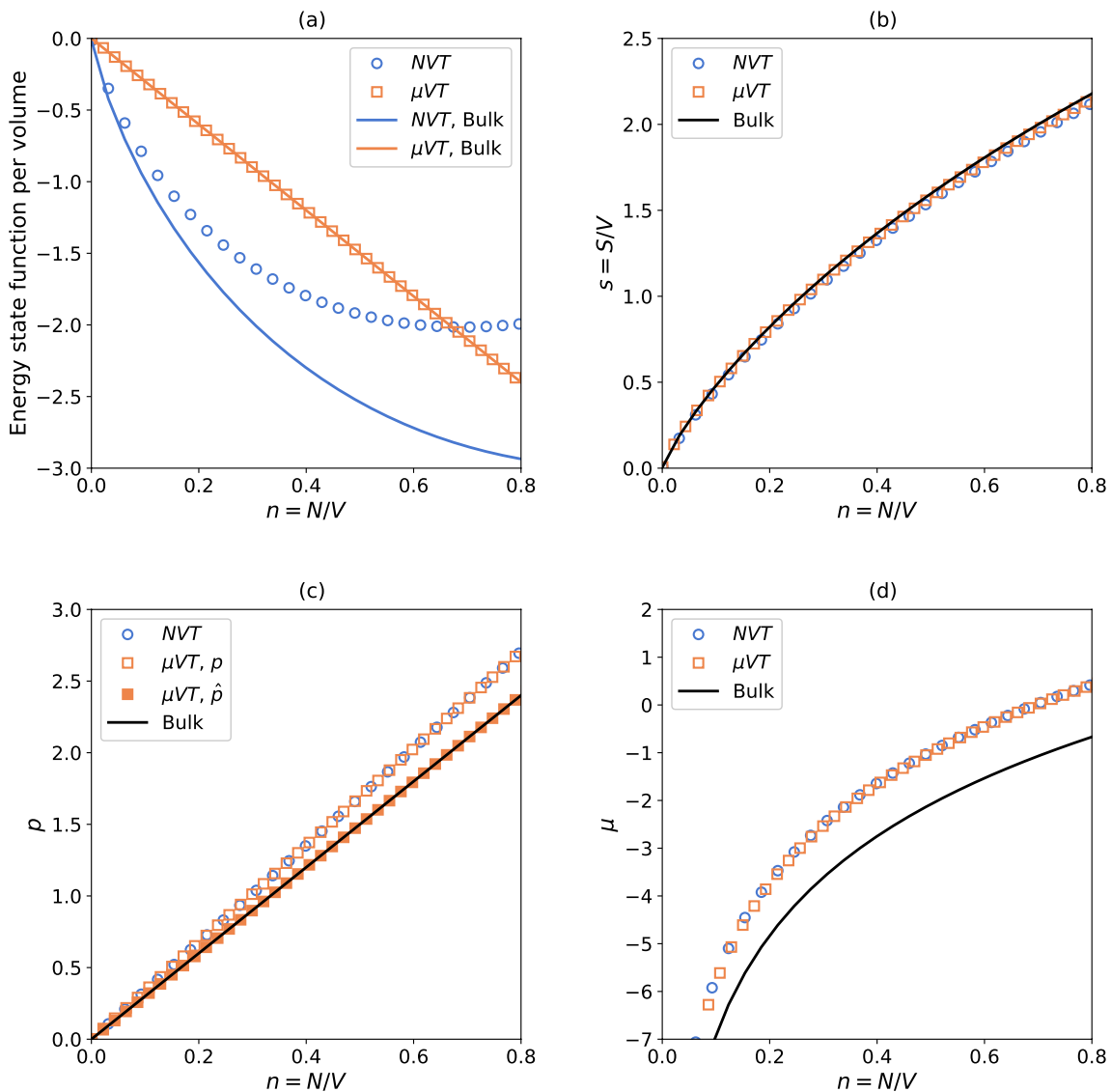


FIG. 4. Energy state functions, entropy, pressure and chemical potential as a function of number density of an ideal gas in a small cubic box with sides  $L = 5$ . The surface energy is  $U^s = 1$  and is experienced by all particles within a distance  $\delta = 1$  from each wall.

this size, the difference between the properties in the two ensembles is barely visible. Further increasing the size of the system gives properties that are visually indistinguishable for the ranges on the y-axis considered here.

The subdivision potential is a central property of the nanothermodynamic description presented by Hill's<sup>26</sup>. Equations (1)-(3) show that when the subdivision potential is zero, the nanothermodynamic description reduces to the macroscopic thermodynamic equations. The concept of the subdivision potential has received much attention in attempts to describe the thermodynamics of small systems<sup>28,44,45</sup>. However, with the exception of the work on spherical adsorbents by Strøm, Bedeaux, and Schnell<sup>45</sup>, its numerical values are usually not pre-

sented. For the ideal gas systems with size  $L = 3$  and  $L = 5$  the subdivision potential is shown in Fig. 5, where we can see that this property is also ensemble dependent.

The equations and figures presented in this section show that an ideal gas in a cubic box is ensemble in-equivalent when the number of particles is small enough. It is in general not possible to give an universal limit for when  $N$  is small enough for these differences to become significant. The model presented here is one example of an ideal gas system that can be used to investigate finite size effects of this kind. Similar models can be derived for other geometries and dimensions, which can affect the magnitude of the surface terms, and thereby change the relative importance of the factorial



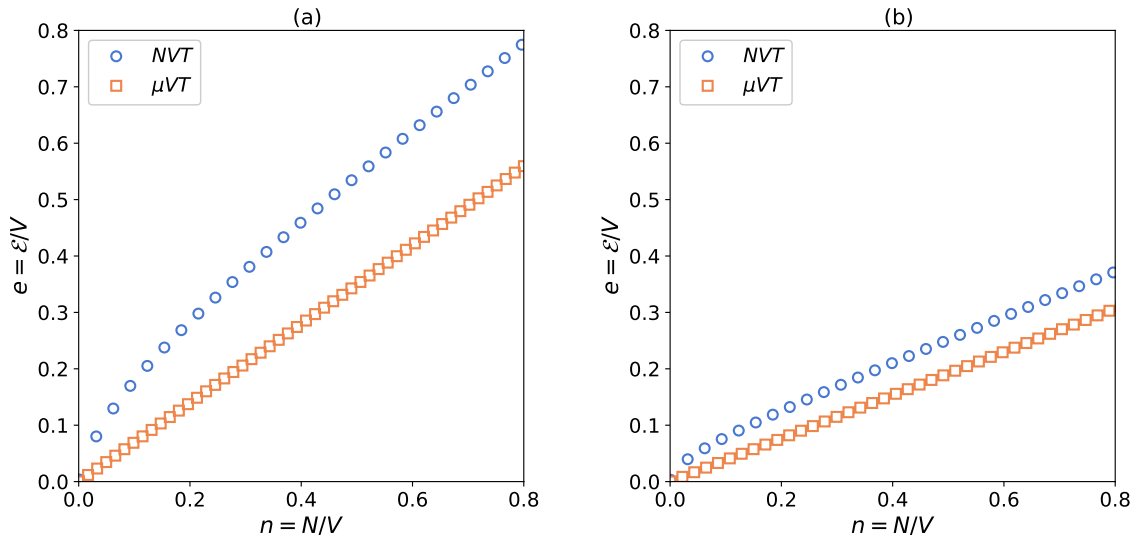


FIG. 5. Subdivision potential as a function of number density of an ideal gas in a small cubic box with sides (a)  $L = 3$  and (b)  $L = 5$ . The surface energy is  $U^s = 1$  and is experienced by all particles within a distance  $\delta = 1$  from each wall.

terms. The magnitude of the surface terms depends on the number of particles, the size and shape,  $U^s$  and  $\delta$ , while the magnitude of the factorial terms depends only on the number of particles. However, the relative influence of the factorial terms will of course depend on the size and shape,  $U^s$  and  $\delta$ .

Some general remarks that can be made are that the ensemble in-equivalence of the ideal gases does not depend on the surface energy, as long as this surface energy does not depend on  $N$ ,  $\mu$ ,  $V$  or  $T$ . It is also not a result of long-range interactions since the ideal gas particles have no inter-particle interactions. In the next section, we investigate how the results for the ideal gases can be used to gain insight into the ensemble equivalence for open and closed small systems with interacting particles.

## B. Interacting particles

In this section, we investigate the properties of open and closed systems computed from MC simulations. Before we compare these results with the ones predicted by the ideal gas model, we discuss different methods for computation of average values in small systems. Error bars corresponding to two standard deviations are included in all figures with markers, but they are smaller than the marker size.

### 1. Computing averages in small systems

The macroscopic definitions used for computation of thermodynamic properties from simulations do not always apply to small systems<sup>44</sup>. One of the reasons for this is that the volume is often not uniquely defined for systems with signif-

icant surface effects. For homogeneous systems with periodic boundary conditions, the volume available to the center of masses of the molecules is equal to the full volume of the simulation box. For small, confined systems, these two volumes often differ, which can affect the computation of the properties that depend on the system's volume. How to get a proper representation of volume dependent properties has been widely discussed, and new methods have been proposed for computation of both the pressure and the density of small systems<sup>20,27,28,49</sup>. The definition of system volume will clearly also affect the properties presented in this work. However, it should not affect the comparison between the properties in open and closed systems as long as their volumes are equally defined.

Something that can affect this comparison is the method used for computation of mean values. For the open system, two ways of computing the mean density are compared. The first is the *arithmetic mean*, which is the sum of all the sampled values, divided by the number of sampled values. This is also referred to as the average, or the sample mean. Another alternative is the *population mean*, or expected value, which is the number that is most likely to be observed during the simulations. For large systems, these two ways of computing the mean value should be equivalent. For small systems however, the density distributions of the open system will have a cut-off at low densities, since we cannot have a number of particles below zero.

In order to investigate how this influences the comparison of the properties in open and closed systems, we compare the two methods for the LJ systems with  $U^s = 1$ . Figure 6, which displays some selected density distributions for this system with size  $L = 3$ , illustrates this effect. The population mean is extracted from the dashed lines, which are computed by fitting

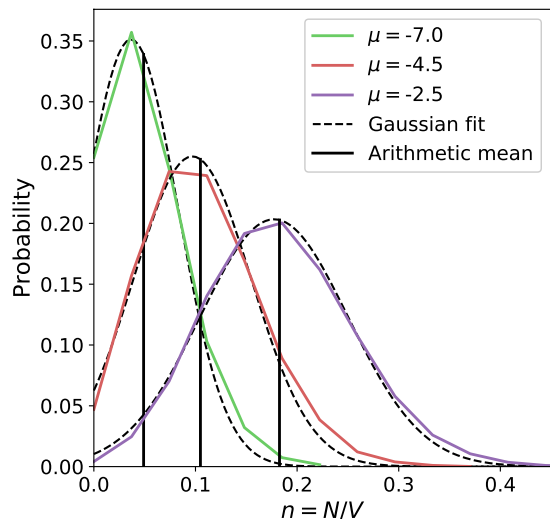


FIG. 6. Distribution of number density for a system with LJ particles for a few selected chemical potentials, in a system with  $L = 3$ . The surface energy is  $U^s = 1$  and is experienced by all particles within a distance  $\delta = 1$  from each wall.

a Gaussian curve to the distributions. For extracting the population mean, two different methods of curve fitting are tested. In the first method, all data points from the density distributions are included in the fit, while in the second approach, we include only the data points that are available symmetrically around the maximum value of each distribution. The two methods are found to give the same results within the statistical accuracies, and we therefore only present the population mean densities extracted from the symmetrical fit.

The solid black lines in Fig. 6 represent the arithmetic mean, which clearly do not fit the peaks of the distributions for low densities. It is also clear that the Gaussian curves do not fit the distributions perfectly, but instead are shifted towards lower densities. The population mean density becomes lower than the arithmetic mean density, and the comparison of the properties in the open and closed systems are clearly influenced by the method used to compute the mean density.

This also becomes clear from Fig. 7, which shows the pressure and the chemical potential as functions of the density for small open and closed LJ systems with size  $L = 3$  and  $U^s = 1$ . In the low density region, the difference between the densities computed from the arithmetic mean and the ones computed from the population mean is visible. For high densities, the two methods give overlapping densities.

Both methods still show that there is a difference between the chemical potentials in open and closed systems, and that the trend is similar to that predicted by the ideal gas model in Fig. 3. Figure 7 (a) also shows a slight difference between the pressures at higher densities, which is a feature not described by the ideal gas model. Since the main focus of this section is to investigate the differences between the arithmetic mean and the population mean, we discuss the deviations from the

ideal gas model in more detail in the next section.

Figure 8 shows the pressure and the chemical potential as functions of density in open and closed systems with size  $L = 5$ . Already at this size, the mean densities are close to indistinguishable in the figure.

For better visualization of the difference between the properties in open and closed systems, we fit a quadratic spline function to the data points displayed in Figs. 7-8, and the other investigated system sizes ( $L = 7, 9$ ), as well as the system with PBCs. Since the spacing between the data points on the y-axis is increasing in the high density region for the pressure, and in the low density region for the chemical potential, we fit the spline functions only to the densities between  $n = 0.1 - 0.7$ , in order to reduce the chance of overfitting. The differences between the properties in the open and closed systems, based on these spline functions, are shown in Fig. 9 for the pressure, and in Fig. 10 for the chemical potential. The predictions of the ideal gas model, shown in Tables I and II, are also included in the figure.

Also here we see a clear difference between mean density computed by the arithmetic mean and the one computed by the population mean, as they give different trends as functions of the density. For both properties, the population mean gives less systematic results, and display larger fluctuations than those found by using the arithmetic mean. As Fig. 6 indicates, neither of the methods perfectly describe the expected number of particles. The arithmetic mean does not fit the peak of the distribution, and the Gaussian curve, used to extract the population mean, does not fit the tails of the distribution. Due to the additional curve fitting step, the population mean becomes the less convenient method among the two. When we have such a low number of data points available, curve fitting can quickly induce errors. In the following, we therefore consider only the results represented by the arithmetic mean density.

## 2. Properties in open and closed systems with interacting particles

In this section we investigate how the pressure and the chemical potential differ in open and closed systems for all different boundary conditions and particle types investigated by simulations. The results presented in the last section already show that the properties in open and closed systems are different when the systems are small enough. Comparing Figs. 3 (c) and (d) to Fig. 7 for size  $L = 3$ , and Figs. 4 (c) and (d) to Fig. 8 for size  $L = 5$ , shows that in the low density region, the pressure and chemical potential of the interacting systems are similar to the values predicted by the ideal gas model. For the more dense systems, where the effects of crowding and cooperativity becomes important, we see larger differences. Figures showing computed values for all systems sizes, types of boundary conditions, and particle interactions are found in the SM.

Figures 9-10 show that the differences between the properties in the open and closed systems cannot be fully explained by the ideal gas model. For the chemical potential difference,

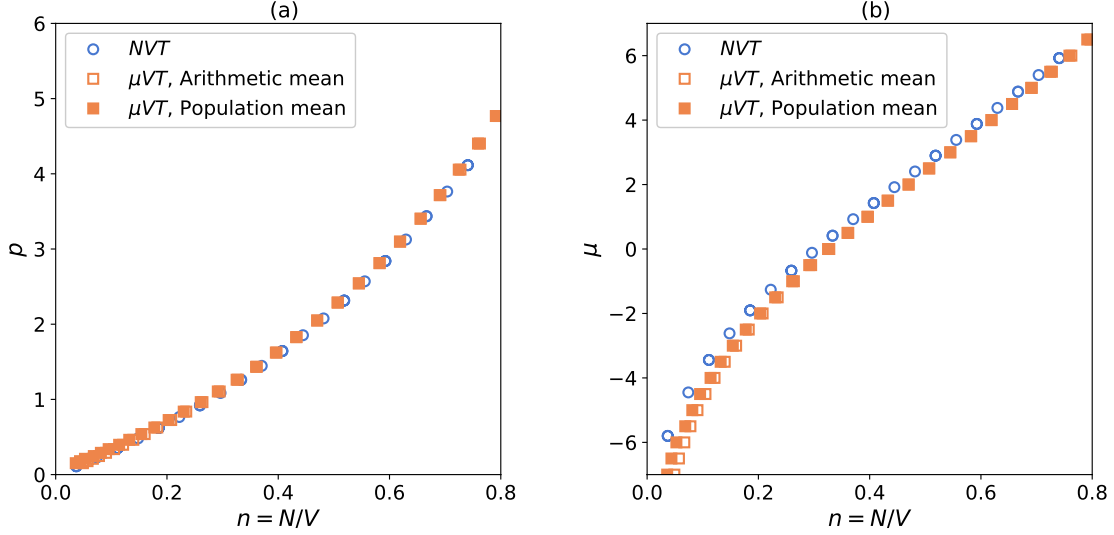


FIG. 7. Pressure and chemical potential as a function of number density of a LJ fluid in a small cubic box with sides  $L = 3$ , computed from MC simulations. The surface energy is  $U^s = 1$  and is experienced by all particles within a distance  $\delta = 1$  from each wall.

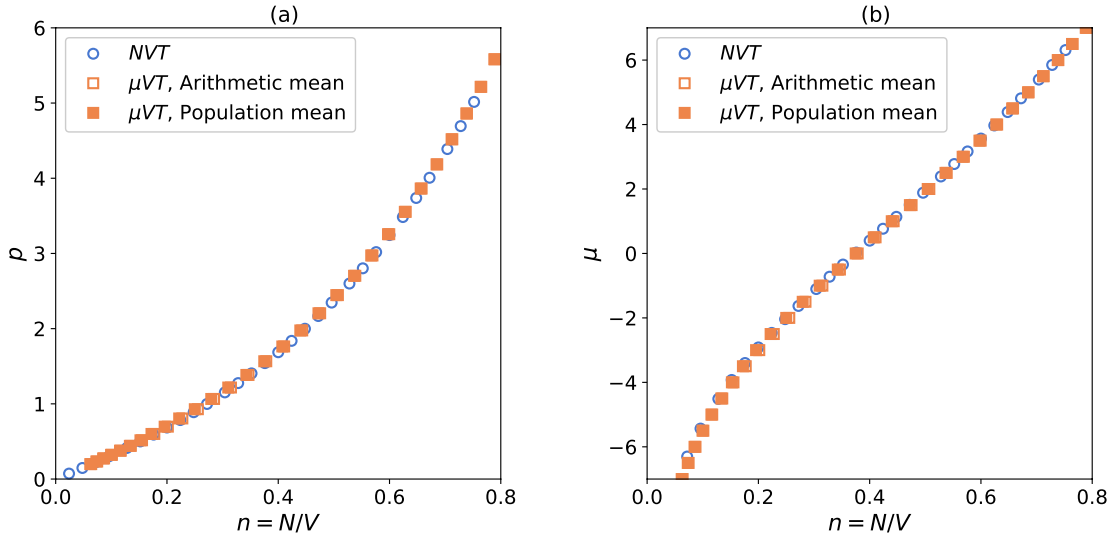


FIG. 8. Pressure and chemical potential as a function of number density of a LJ fluid in a small cubic box with sides  $L = 5$ , computed from MC simulations. The surface energy is  $U^s = 1$  and is experienced by all particles within a distance  $\delta = 1$  from each wall.

the trend of the interacting particles is very similar to the one predicted by the ideal gas model, which could indicate that this difference is partly described by the factorial terms. The contributions from the interactions between the particles can be investigated separately by subtracting the ideal gas prediction from the total property computed from simulations. To directly compare the magnitude of this contribution for the pressure and the chemical potential, the properties need to be evaluated for the same units. We therefore consider the con-

jugate pairs in the expression for the internal energy of the system, divided by the volume

$$u = sT - p + \mu n, \quad (19)$$

where  $u = U/V$  and  $s = S/V$ .

The differences investigated are

$$\begin{aligned} \Delta(-p) &= \Delta(-p)_{\text{IG}} + \Delta(-p)_{\text{int}} \\ &= [(-p(N, V, T)) - (-p(\mu, V, T))]_{\text{IG}} \\ &\quad + [(-p(N, V, T)) - (-p(\mu, V, T))]_{\text{int}}, \quad (20) \end{aligned}$$

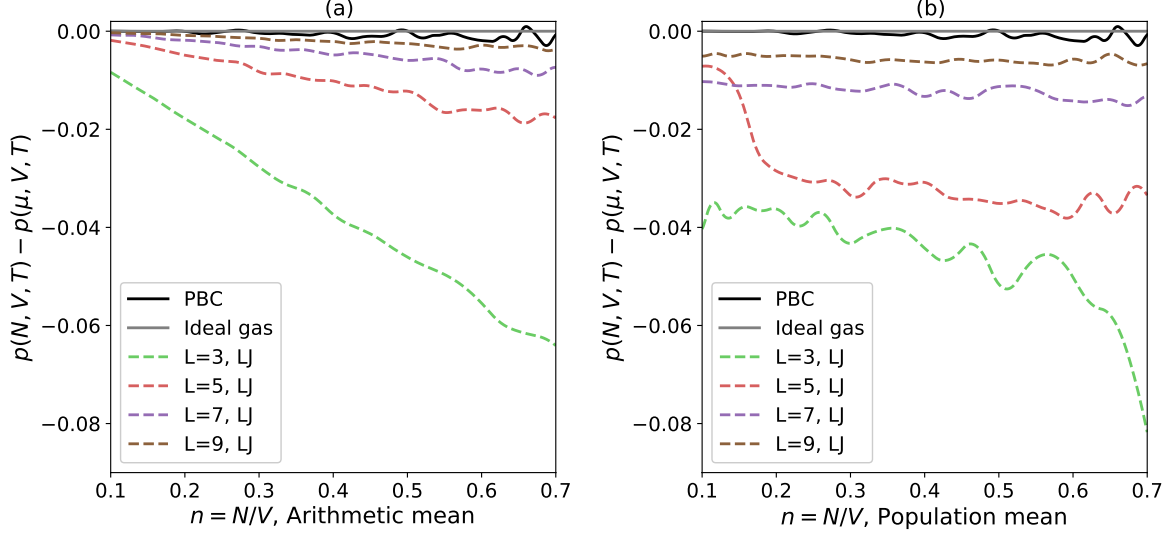


FIG. 9. How the difference in pressure of a LJ fluid in open and closed systems vary with arithmetic mean density (a) and population mean density (b), for differently sized small cubic boxes. The surface energy is  $U^s = 1$  and is experienced by all particles within a distance  $\delta = 1$  from each wall.

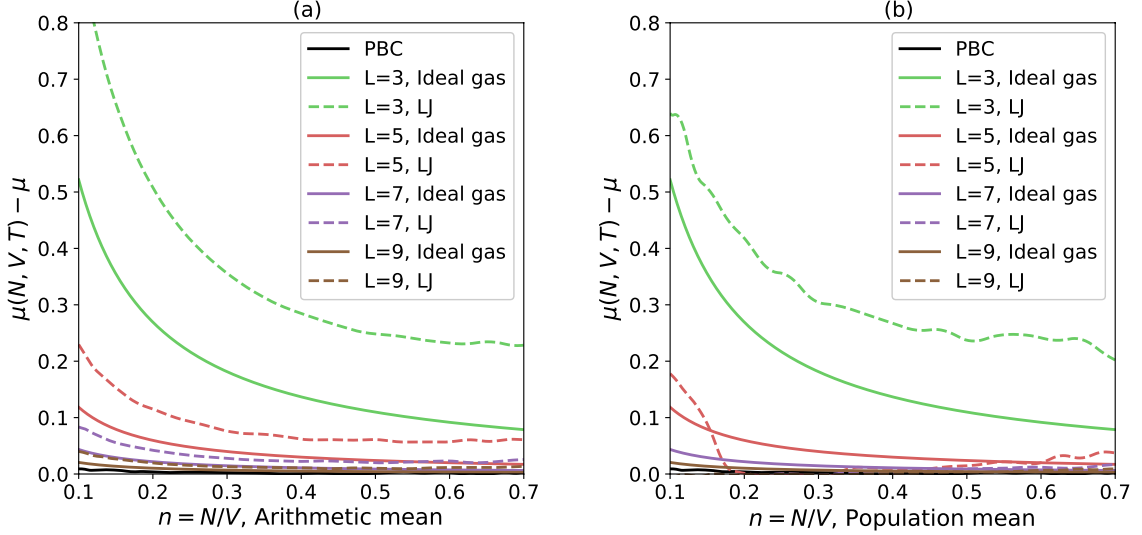


FIG. 10. How the difference in chemical potential of a LJ fluid in open and closed systems vary with arithmetic mean density (a) and population mean density (b), for differently sized small cubic boxes. The surface energy is  $U^s = 1$  and is experienced by all particles within a distance  $\delta = 1$  from each wall.

and

$$\begin{aligned} \Delta(\mu n) &= \Delta(\mu n)_{\text{IG}} + \Delta(\mu n)_{\text{int}} \\ &= [\mu(N, V, T)n - \mu n(\mu, V, T)]_{\text{IG}} \\ &\quad + [\mu(N, V, T)n - \mu n(\mu, V, T)]_{\text{int}}, \end{aligned} \quad (21)$$

where the subscript "IG" refers to the ideal gas contribution, and "int" refers to the contribution from particle interactions. This is often also referred to as the residual contribution.

Figure 11 shows  $\Delta(-p)$  and  $\Delta(\mu n)$  for the four different sizes investigated for the system with LJ particles and  $U^s = 1$ . The values of  $\Delta(-p)$  show clear linear trends for all system sizes, while the values of  $\Delta(\mu n)$  are almost constant for low densities, with an increasing slope at higher densities. The ideal gas contribution to these properties show very little dependence on density:  $\Delta(-p)_{\text{IG}} = 0$ , while Eq. (18) shows that  $\Delta(\mu n)_{\text{IG}}$  is approximately constant for different densities

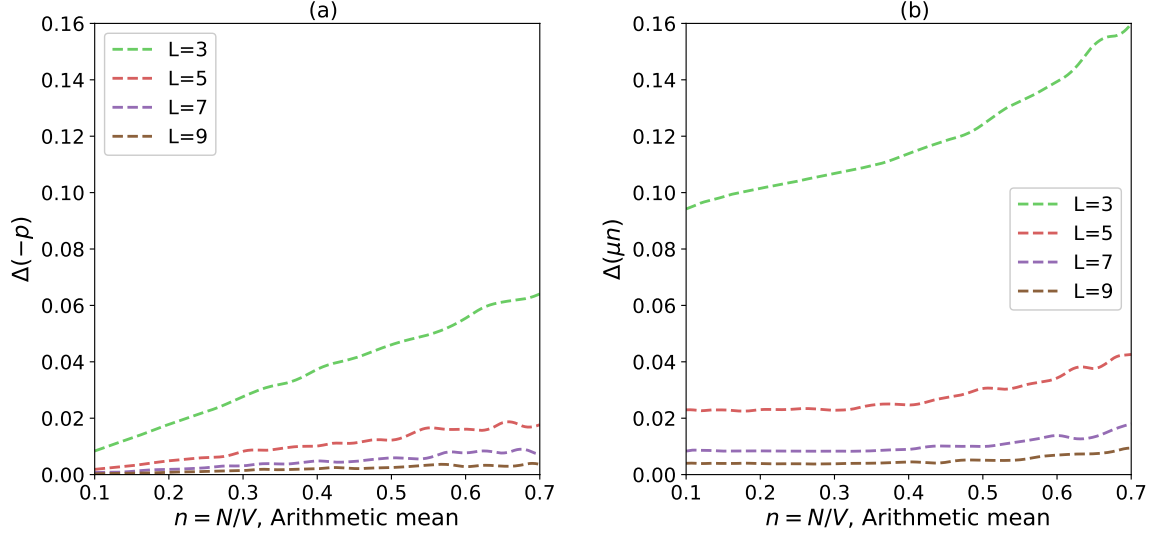


FIG. 11. How the difference in pressure (a) and the chemical potential (b), in open and closed systems, minus the prediction of the ideal gas model from Tables I-II, vary with density. The simulation box sizes are  $L = 3, 5, 7, 9$ . The particles are interacting through the truncated and shifted LJ potential, the surface energy is  $U^s = 1$  which is experienced by all particles within a distance  $\delta = 1$  from each wall.

when the volume is constant. The density dependence shown in Fig. 11 must therefore be related to contribution from the particle interactions,  $\Delta(-p)_{\text{int}}$  and  $\Delta(\mu n)_{\text{int}}$ .

This contribution becomes more important at higher densities, which could indicate that it is related to the particles' excluded volume. The excluded volume of a particle is the volume that is inaccessible to other particles in the system due to the presence of the first particle. At higher densities, a larger portion of the system will be occupied by the particles' excluded volume. At low densities, where the particles are more free to move around, this effect is less prominent. This is similar to the results found from simulations of stretching of polymer chains performed by Bering *et al.*<sup>29</sup>. In the comparison between isomeric and isotensional stretching, they find that for small forces, the molecules are in what they call an entropic regime. In this regime, the molecule has numerous degrees of freedom for movements, and the system is ensemble equivalent. As the molecule becomes more stretched out, the properties computed in the isomeric and the isotensional ensembles start to differ. This could indicate that restricted movement of particles is related to ensemble in-equivalence. We further explore this by investigating the effect of changing the interactions between the particles and the wall, and the effect of changing the interparticle interactions.

First, we investigate how the value of the surface energy,  $U^s$ , influences the difference between the properties in the open and closed systems. Higher values of  $U^s$  means that the particles are less likely to be positioned close to the system walls. For better readability, the following figures only show the results of the two smallest systems. Figure 12 shows how  $\Delta(-p)$  and  $\Delta(\mu n)$  depend on the density for  $U^s = 0$ ,  $U^s = 1$  and  $U^s = 3$ . As the surface energy is increasing, the values

of  $\Delta(\mu n)$  become larger. For the pressure, however, the difference still show a linear trend, but it is not increasing with  $U^s$ . As  $U^s$  becomes larger, these lines instead show a slight decrease in the slope, and an increase in the intersection with the y-axis.

By changing the interparticle interactions, the excluded volume also changes. The WCA potential consists of only the repulsive part of the LJ potential, and will therefore have a larger excluded volume. Figure 13 compares the values of  $\Delta(-p)$  and  $\Delta(\mu n)$  for the LJ systems and the WCA systems with  $U^s = 0$ . This figure shows that the effect of a larger excluded volume is similar to increased repulsive forces close to the walls. The values of  $\Delta(\mu n)$  are larger for the WCA systems than they are for the LJ systems, and the change in the slope of  $\Delta(-p)$  is more visible in this plot.

This indicates that, for the systems investigated here, the contribution from particle interactions to the difference between the properties in open and closed systems are related to restrictions in movement of particles. As the movements of the particles become more restricted, the difference in the chemical potential shows a stronger dependence on density. The pressure, on the other hand becomes less dependent on density, and is instead approaching a constant value. At this stage, it is unclear why  $\Delta(-p)$  and  $\Delta(\mu n)$  respond differently to these changes. It is possible that the pressure difference is affected by crowding and cooperativity in a way that is not described by the restriction in movement of the particles alone. Or, it could be related to the fact that  $N$  is a canonical variable and  $\mu$  is a grand canonical variable, while  $p$  is neither a canonical nor a grand canonical variable. This can be further studied by investigating the effect of restrictions in particle movement for pairs of ensemble variables of other dual sta-

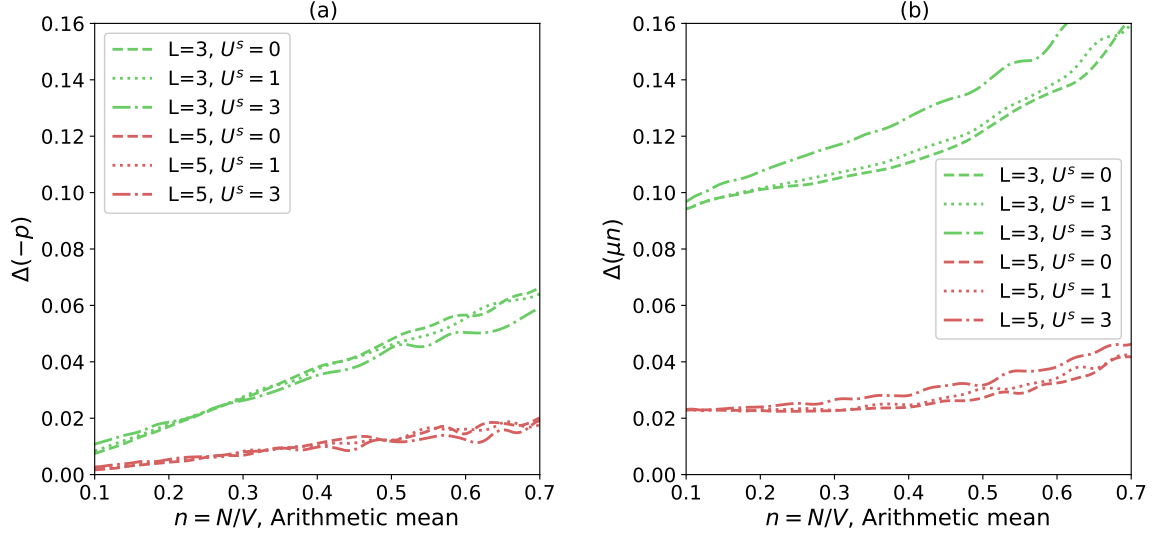


FIG. 12. How the difference between pressure (a) and the chemical potential (b), in open and closed systems vary with density. The simulation box sizes are  $L = 3, 5$ . The particles are interacting through the truncated and shifted LJ potential, the surface energy is  $U^s = 0$  (dashed),  $U^s = 1$  (dotted) or  $U^s = 3$  (dash-dot), which is experienced by all particles within a distance  $\delta = 1$  from each wall.

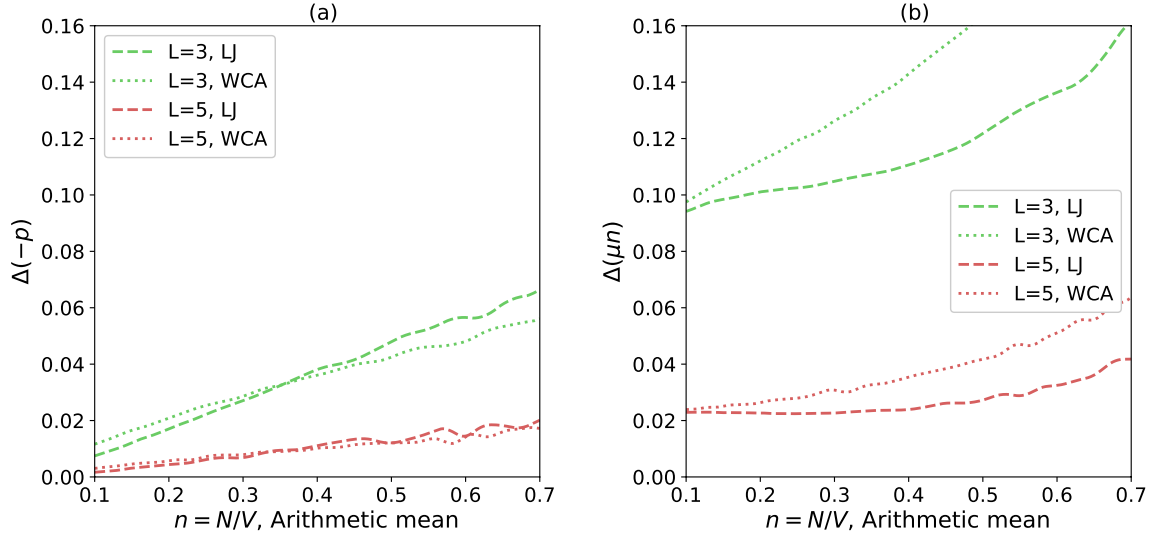


FIG. 13. How the difference between pressure (a) and the chemical potential (b) in open and closed systems vary with density. The particles are interacting through the truncated and shifted LJ potential (dashed), or the WCA potential (dotted). The simulation box sizes are  $L = 3, 5$ . There is no surface energy ( $U^s = 0$ ).

tistical ensembles, such as the  $U$  and  $T$  in the microcanonical and canonical ensemble, or  $V$  and  $p$  in the canonical and the isobaric-isothermal ensemble. However, this falls beyond the scope of the present work.

## VI. CONCLUSION

The thermodynamics of small systems is known to deviate from the classical behavior. One consequence of this is that the properties can become ensemble dependent. We investigate the ensemble equivalence of open (grand canonical) and closed (canonical) ensembles for small systems contain-

ing ideal gas particles, and for systems containing particles interacting via either the LJ or the WCA potentials.

Ideal gas systems are investigated analytically by deriving the properties from the respective partition functions. A surface contribution is introduced to the ideal gas particles' potential energy through a surface energy  $U^s$  experienced by particles closer than a distance  $\delta$  from each wall. The purpose of this is to investigate whether the behavior of a simple model system can provide insight into the ensemble in-equivalence of more complex systems with interacting particles. For the ideal gas, we find that the properties in open and closed ensembles are not equivalent. The ensemble in-equivalence is not a consequence of the surface energy since the surface contribution to the ideal gas properties is equivalent in the open and closed systems. The difference between the properties of the ideal gas in the open and closed systems is instead a result of factorial terms that appear in the properties of the closed system. These terms depend only on the number of particles, and are direct consequences of avoiding assumptions about  $N \rightarrow \infty$ , such as Stirling's approximation.

The systems with interacting particles are investigated through MC simulations. For small number of particles, the systems investigated through simulations have different pressures and chemical potentials in the open and closed systems. We find that the magnitude of the difference between the properties in the open and closed systems of a given volume depends on the surface energy  $U^s$ , the interatomic interactions, and the density. This deviates from the prediction of the difference between the properties in the open and closed systems of the ideal gas, which for a given volume is independent of  $U^s$  and approximately independent of density. For the interacting particles, we also find that increasing the particles' excluded volume, and increasing the repulsive forces close to the walls, results in similar responses in the differences between properties in open and closed systems. This indicates that the contribution to ensemble in-equivalence, which is not explained by the ideal gas model, is connected to the restricted movement of particles in the systems, and that system features which increase this restriction can lead to larger differences between the properties in the open and closed systems.

## SUPPLEMENTARY MATERIAL

See supplementary material for full derivation of the properties of the ideal gases, and the computed thermodynamic properties for all systems investigated through simulations.

## DATA AVAILABILITY STATEMENT

The data that support the findings of this study are available from the corresponding author upon reasonable request.

## AUTHOR DECLARATIONS

The authors have no conflicts to disclose.

## ACKNOWLEDGMENTS

This work is supported by the Research Council of Norway (275754). Computational resources are provided by the UNINETT Sigma2 - The National Infrastructure for High Performance Computing and Data Storage in Norway (NN9414k).

- <sup>1</sup>D. Frenkel and B. Smit, *Understanding Molecular Simulation*, second edition ed. (Academic Press, 2002).
- <sup>2</sup>I. Oppenheim and P. Mazur, "Density expansions of distribution functions. i.: Virial expansion for finite closed systems: Canonical ensemble," *Physica*. **23**, 197–215 (1957).
- <sup>3</sup>J. L. Lebowitz and J. K. Percus, "Long-range correlations in a closed system with applications to nonuniform fluids," *Phys. Rev.* **122**, 1675–1691 (1961).
- <sup>4</sup>J. L. Lebowitz and J. K. Percus, "Thermodynamic properties of small systems," *Phys. Rev.* **124**, 1673–1681 (1961).
- <sup>5</sup>J. I. Siepmann, I. R. McDonald, and D. Frenkel, "Finite-size corrections to the chemical potential," *J. Phys. Condens. Matter*. **4**, 679–691 (1992).
- <sup>6</sup>P. Krüger, S. K. Schnell, D. Bedeaux, S. Kjelstrup, T. J. H. Vlugt, and J.-M. Simon, "Kirkwood–buff integrals for finite volumes," *J. Phys. Chem. Lett.* **4**, 235–238 (2013).
- <sup>7</sup>J. Milzetti, D. Nayar, and N. F. A. van der Vegt, "Convergence of kirkwood–buff integrals of ideal and nonideal aqueous solutions using molecular dynamics simulations," *J. Phys. Chem. B*. **122**, 5515–5526 (2018).
- <sup>8</sup>N. Dawass, P. Krüger, S. K. Schnell, J.-M. Simon, and T. J. H. Vlugt, "Kirkwood–buff integrals from molecular simulation," *Fluid Ph. Equilibria*. **486**, 21 – 36 (2019).
- <sup>9</sup>W. W. Wood, F. R. Parker, and J. D. Jacobson, "Recent monte carlo calculations of the equation of state of lenard-jones and hard sphere molecules," *Il Nuovo Cimento*. **9**, 133–143 (1958).
- <sup>10</sup>B. J. Alder and T. E. Wainwright, "Studies in molecular dynamics. ii. behavior of a small number of elastic spheres," *J. Chem. Phys.* **33**, 1439–1451 (1960).
- <sup>11</sup>K. Binder, "Finite size scaling analysis of ising model block distribution functions," *Z. Phys.* **43**, 119–140 (1981).
- <sup>12</sup>M. Rovere, P. Nielaba, and K. Binder, "Simulation studies of gas-liquid transitions in two dimensions via a subsystem-block-density distribution analysis," *Z. Phys.* **90**, 215–228 (1993).
- <sup>13</sup>S. K. Schnell, T. J. H. Vlugt, J.-M. Simon, D. Bedeaux, and S. Kjelstrup, "Thermodynamics of a small system in a  $\mu t$  reservoir," *Chem. Phys. Lett.* **7504**, 199 – 201 (2011).
- <sup>14</sup>S. K. Schnell, T. J. H. Vlugt, J.-M. Simon, D. Bedeaux, and S. Kjelstrup, "Thermodynamics of small systems embedded in a reservoir: a detailed analysis of finite size effects," *Mol. Phys.* **110**, 1069–1079 (2012).
- <sup>15</sup>P. Ganguly and N. F. A. van der Vegt, "Convergence of sampling kirkwood–buff integrals of aqueous solutions with molecular dynamics simulations," *J. Chem. Theory Comput.* **9**, 1347–1355 (2013).
- <sup>16</sup>R. Cortes-Huerto, K. Kremer, and R. Potestio, "Communication: Kirkwood–buff integrals in the thermodynamic limit from small-sized molecular dynamics simulations," *J. Chem. Phys.* **145**, 141103 (2016).
- <sup>17</sup>M. Heidari, K. Kremer, R. Potestio, and R. Cortes-Huerto, "Fluctuations, finite-size effects and the thermodynamic limit in computer simulations: Revisiting the spatial block analysis method," *Entropy*. **20**, 222 (2018).
- <sup>18</sup>M. Heidari, K. Kremer, R. Potestio, and R. Cortes-Huerto, "Finite-size integral equations in the theory of liquids and the thermodynamic limit in computer simulations," *Mol. Phys.* **116**, 3301–3310 (2018).
- <sup>19</sup>B. A. Strøm, J.-M. Simon, S. K. Schnell, S. Kjelstrup, J. He, and D. Bedeaux, "Size and shape effects on the thermodynamic properties of nanoscale volumes of water," *Phys. Chem. Chem. Phys.* **19**, 9016–9027 (2017).
- <sup>20</sup>V. Bråten, Ø. Wilhelmsen, and S. K. Schnell, "Chemical potential differences in the macroscopic limit from fluctuations in small systems," *J. Chem. Inf. Model.* **61**, 840–855 (2021).
- <sup>21</sup>W. H. Roos, I. L. Ivanovska, A. Evilevitch, and G. J. L. Wuite, "Viral capsids: Mechanical characteristics, genome packaging and delivery mechanisms," *Cell. Mol. Life Sci.* **64**, 1484 (2007).



- <sup>22</sup>N. P. Stone, G. Demo, E. Agnello, and B. A. Kelch, “Principles for enhancing virus capsid capacity and stability from a thermophilic virus capsid structure,” *Nat. Commun.* **10**, 4471 (2019).
- <sup>23</sup>M. Kulmala, H. Vehkamäki, T. Petäjä, M. Dal Maso, A. Lauri, V.-M. Kerminen, W. Birmili, and P. McMurry, “Formation and growth rates of ultrafine atmospheric particles: a review of observations,” *J. Aerosol Sci.* **35**, 143–176 (2004).
- <sup>24</sup>H. Singh and R. S. Myong, “Critical review of fluid flow physics at micro-to nano-scale porous media applications in the energy sector,” *Adv. Mater. Sci. Eng.* **2018**, 9565240 (2018).
- <sup>25</sup>P. Sudarsanam, E. Peeters, E. V. Makshina, V. I. Parvulescu, and B. F. Sels, “Advances in porous and nanoscale catalysts for viable biomass conversion,” *Chem. Soc. Rev.* **48**, 2366–2421 (2019).
- <sup>26</sup>T. L. Hill, “Thermodynamics of small systems,” *J. Chem. Phys.* **36**, 3182–3197 (1962).
- <sup>27</sup>O. Galteland, D. Bedeaux, B. Hafskjold, and S. Kjelstrup, “Pressures inside a nano-porous medium. the case of a single phase fluid,” *Front. Phys.* **7**, 60 (2019).
- <sup>28</sup>M. T. Rauter, O. Galteland, M. Erdős, O. A. Moulton, T. J. H. Vlugt, S. K. Schnell, D. Bedeaux, and S. Kjelstrup, “Two-phase equilibrium conditions in nanopores,” *Nanomaterials.* **10** (2020).
- <sup>29</sup>E. Bering, S. Kjelstrup, D. Bedeaux, J. M. Rubi, and A. S. de Wijn, “Entropy production beyond the thermodynamic limit from single-molecule stretching simulations,” *J. Phys. Chem. B.* **124**, 8909–8917 (2020).
- <sup>30</sup>E. Bering, D. Bedeaux, S. Kjelstrup, A. S. de Wijn, I. Latella, and J. M. Rubi, “A legendre–fenchel transform for molecular stretching energies,” *Nanomaterials.* **10** (2020).
- <sup>31</sup>A. Campa, T. Dauxois, and S. Ruffo, “Statistical mechanics and dynamics of solvable models with long-range interactions,” *Phys. Rep.* **480**, 57–159 (2009).
- <sup>32</sup>D. F. A. Campa, T. Dauxois and S. Ruffo, *Physics of Long-Range Interacting Systems* (Oxford University Press, 2014).
- <sup>33</sup>J. M. Rubi, D. Bedeaux, and S. Kjelstrup, “Thermodynamics for single-molecule stretching experiments,” *J. Phys. Chem. B.* **110**, 12733–12737 (2006).
- <sup>34</sup>H. Touchette, R. S. Ellis, and B. Turkington, “An introduction to the thermodynamic and macrostate levels of nonequivalent ensembles,” *Phys. A: Stat. Mech. Appl.* **340**, 138–146 (2004).
- <sup>35</sup>H. Touchette, “Ensemble equivalence for general many-body systems,” *EPL (Europhysics Letters)* **96**, 50010 (2011).
- <sup>36</sup>A. Campa, L. Casetti, I. Latella, A. Pérez-Madrid, and S. Ruffo, “Concavity, response functions and replica energy,” *Entropy.* **20** (2018).
- <sup>37</sup>F. L. Román, A. González, J. A. White, and S. Velasco, “Fluctuations in the number of particles of the ideal gas: A simple example of explicit finite-size effects,” *Am. J. Phys.* **67**, 1149–1151 (1999).
- <sup>38</sup>D. Villamaina and E. Trizac, “Thinking outside the box: fluctuations and finite size effects,” *Eur. J. Phys.* **35**, 035011 (2014).
- <sup>39</sup>M. E. Tuckerman, *Statistical Mechanics: Theory and Molecular Simulation* (Oxford University Press Inc., New York, 2010).
- <sup>40</sup>R. B. Shirts, S. R. Burt, and A. M. Johnson, “Periodic boundary condition induced breakdown of the equipartition principle and other kinetic effects of finite sample size in classical hard-sphere molecular dynamics simulation,” *J. Chem. Phys.* **125**, 164102 (2006).
- <sup>41</sup>M. J. Uline, D. W. Siderius, and D. S. Corti, “On the generalized equipartition theorem in molecular dynamics ensembles and the microcanonical thermodynamics of small systems,” *J. Chem. Phys.* **128**, 124301 (2008).
- <sup>42</sup>T. Niiyama, Y. Shimizu, T. R. Kobayashi, T. Okushima, and K. S. Ikeda, “Effect of translational and angular momentum conservation on energy equipartition in microcanonical equilibrium in small clusters,” *Phys. Rev. E* **79**, 051101 (2009).
- <sup>43</sup>E. N. Miranda, “Statistical mechanics of few-particle systems: exact results for two useful models,” *Eur. J. Phys.* **38**, 065101 (2017).
- <sup>44</sup>D. Bedeaux, S. Kjelstrup, and S. K. Schnell, *Nanothermodynamics. General theory* (Porelab publisher, 2020).
- <sup>45</sup>B. A. Strøm, D. Bedeaux, and S. K. Schnell, “Adsorption of an ideal gas on a small spherical adsorbent,” *Nanomaterials.* **11** (2021).
- <sup>46</sup>T. L. Hill, *Thermodynamics of Small Systems* (Dover Publications, New York, 1994).
- <sup>47</sup>J. D. Weeks, D. Chandler, and H. C. Andersen, “Role of repulsive forces in determining the equilibrium structure of simple liquids,” *J. Chem. Phys.* **54**, 5237–5247 (1971).
- <sup>48</sup>B. Widom, “Some topics in the theory of fluids,” *J. Chem. Phys.* **39**, 2808–2812 (1963).
- <sup>49</sup>H. Reiss and D. Reguera, “Understanding the limitations of the virial in the simulation of nanosystems: A puzzle that stimulated the search for understanding,” *J. Phys. Chem. B.* **108**, 6555–6563 (2004).